Reduced-Size LHD-Type Fusion Reactor with D-Shaped Magnetic Surface[*]

Tsuguhiro WATANABE

National Institute for Fusion Science, Toki 509-5292, Japan

A new winding law for the continuous helical coils is proposed for Large Helical Device (LHD) type fusion reactors to satisfy the requirements for a wide blanket space and large plasma volume. Helical coils wound along the geodesic line of a torus with an elongated cross section can produce a magnetic configuration having a D-shaped magnetic surface with a magnetic well in the core region and high magnetic shear in the peripheral regions. The DT alpha particle confinement performance is greatly improved by increasing the elongation factor κ of the cross section of the winding frame for the helical coils. The results suggest that a smaller LHD-type fusion reactor can be realized.

© 2012 The Japan Society of Plasma Science and Nuclear Fusion Research

1. Introduction

A Large Helical Device (LHD) type magnetic configuration ($\ell = 2$ heliotron configuration) is produced by continuous helical and vertical coil systems. The LHD experiments have achieved an average beta value of 5% without beta collapse.

The LHD helical coils are wound as $\chi = p\phi + \alpha_c \sin p\phi$ on a torus with a circular cross section ($R_c = 3.9$ m, $a_c = 0.975$ m), where p is the helical pitch number ($\equiv m/\ell = 5$), and χ and ϕ are the poloidal and toroidal angles, respectively. The coil pitch parameter γ is 1.25 ($\equiv (m/\ell)/(R_c/a_c)$). The helical coil winding of the LHD is shown in Fig. 1 with the vacuum vessel and divertor traces of the lines of force. The small pitch modulation of $\alpha_c = 0.1$ was determined by considering the gap distance between the first wall and the last closed flux surface (LCFS) and the confinement properties of the high-energy particles [1].

High helical symmetry of the magnetic surface with an elliptical cross section and good confinement of high energy particles in the standard LHD configurations have been numerically confirmed [2] (see Figs. 2 and 3 (a)).

High-performance energetic particle confinement was experimentally confirmed by measurements of the high-energy ion tail, which extended up to 1.6 MeV during long-pulse ion cyclotron resonance frequency (ICRF) heating operation of the LHD [3].

In design studies of a LHD-type fusion reactor (a force-free helical reactor (FFHR)), it becomes important to balance the blanket space ($\equiv \delta$: the narrowest space between the chaotic field lines and the inner wall of the heli-
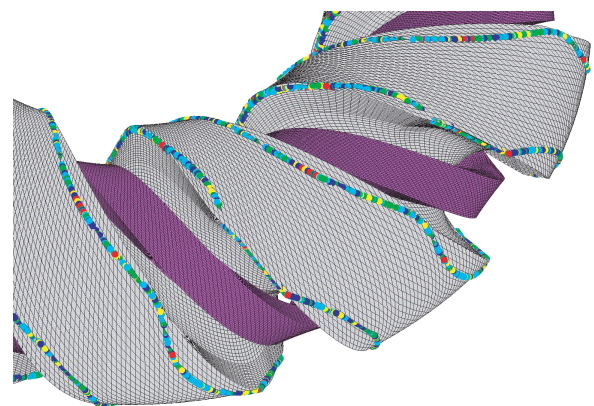

Fig. 1 Vacuum vessel and helical coils of the LHD. Divertor traces are also shown for the configuration of $R_{ax} = 3.65$ m, $\gamma = 1.254$.

cal coils) and the plasma volume. Kozaki pointed out that the γ dependence of the magnetic structure is essential in LHD-type reactors, which is critically sensitive not only for optimizing the plasma volume but also for selecting the optimal blanket conditions [4]. Sufficient blanket space is necessary for adequate tritium breeding and for shielding the magnet. For this purpose, a small γ configuration is preferable, but this reduces the plasma volume.

To simultaneously achieve sufficient blanket space and a large plasma volume in a reduced-size helical reactor, we studied the possibility of a D-shaped LCFS cross section. If the cross section of the magnetic surface becomes concave to the helical coils, it becomes easy to prepare sufficient blanket space. For this purpose, we numerically analyzed the magnetic configuration produced by helical coils wound along a geodesic line on a torus; we refer to the torus as a "winding frame" for the helical coils.
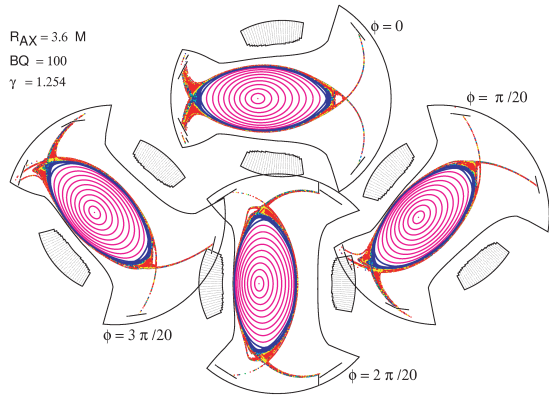
Fig. 2   High symmetry of the LHD magnetic surface. Magnetic surface are plotted in magenta, and chaotic field lines are plotted by red, yellow, green, and blue dots corresponding to the connection length (short to long).
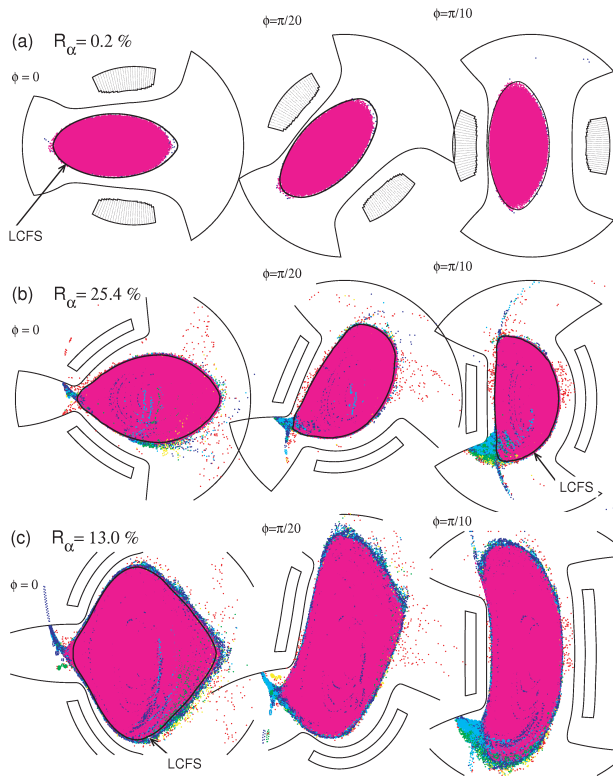

Fig. 3   Performance of a 3.52 MeV alpha particle confinement. Poincaré plots of 3.52 MeV alpha particles generated uniformly inside $\rho/\rho_{\mathrm{lcfs}} \leq 0.8$ with randomly distributed initial pitch angles. Particle number N is 10^3 in (a) and 10^4 in (b) and (c). Black solid curves indicate cross sections of the LCFS as well as the helical coils and vacuum vessel wall. Magenta dots represent confined particles, and lost particles are shown by blue, green, and red dots depending on their lifetimes. Computations were truncated at a maximum of 50 toroidal turns of a 3.52 MeV alpha particle. R_α represents the alpha particle loss rate ($R_0 = 13$ m, $B_{\mathrm{ax}} = 7$ T). (a) standard LHD winding. (b) geodesic winding with weak elongation factor ($\kappa = 1.1$). (c) geodesic winding with strong elongation factor $\kappa = 1.8$.

The effective value of the coil pitch parameter γ along the geodesic line is reduced (increased) inboard (outboard) of the torus. Therefore, sufficient space is reserved between the first wall and the LFCS, and the position of the magnetic axis shifts close to the center of the two helical coils, producing a large plasma volume and forming a magnetic well.

In Sec. 2, we describe the helical winding along the geodesic line on a torus with an elongated cross section. In Sec. 3, the characteristics of the magnetic lines of force produced by the geodesic winding helical coil system are summarized, together with the 3.52 MeV alpha particle confinement performance. We discuss our results in Sec. 4.

2. Geodesic Winding of Helical Coils

Geodesic winding on a toroidal surface with a constant major radius R and a constant minor radius a has been studied for superconducting magnetic energy storage [5] to reduce the electromagnetic stress in coil systems.

We need the tangible shape of the helical coil in order to evaluate the blanket space. Thus, we introduce the reference helical trajectory r_c for the helical coils, similar to the design of the LHD coils and vacuum vessel. We formulated the geodesic winding of the reference helical trajectory on a toroidal surface with a variable major radius $R_c(\chi)$ and a variable minor radius $a(\chi)$ in order to improve the confinement of 3.52 MeV alpha particles.

$$r = a(\chi)\cos\chi + R_c(\chi), \tag{1}$$

$$z = a(\chi)\sin\chi, \tag{2}$$

where r and z are the standard cylindrical coordinates. The reference helical trajectory r_c is given by

$$r_c(\phi) = \{R_c\cos p\phi + a(\chi)\cos(\chi - p\phi)\}\,\boldsymbol{i}$$
$$+ \{-R_c\sin p\phi + a(\chi)\sin(\chi - p\phi)\}\,\boldsymbol{j}, \tag{3}$$

using a helical rotating helical coordinate system [2]. The orbit length L of the reference helical trajectory r_c is given by

$$L = \int_{\pi/2p}^{\pi/2p+2\pi/p} \sqrt{\left(\frac{\mathrm{d}r_c}{\mathrm{d}\phi}\right)^2}\,\mathrm{d}\phi. \tag{4}$$

The Euler equation for the geodesic line is reduced to

$$0 = \delta \int_{\pi/2p}^{\pi/2p+2\pi/p} \sqrt{A^2\left(\frac{\mathrm{d}\chi}{\mathrm{d}\phi}\right)^2 + B^2}\,\mathrm{d}\phi, \tag{5}$$

$$0 = \frac{\mathrm{d}^2\chi}{\mathrm{d}\phi^2} + \left(\frac{A'}{A} - 2\frac{B'}{B}\right)\left(\frac{\mathrm{d}\chi}{\mathrm{d}\phi}\right)^2 - \frac{B\,B'}{A^2}, \tag{6}$$

$$C \equiv a(\chi)\sin\chi, \tag{7}$$

$$B \equiv R_c(\chi) + a(\chi)\cos\chi, \tag{8}$$

$$A \equiv \sqrt{\left(\frac{\mathrm{d}B}{\mathrm{d}\chi}\right)^2 + \left(\frac{\mathrm{d}C}{\mathrm{d}\chi}\right)^2}. \tag{9}$$

Corresponding to the pair of helical coils, there are two

types of boundary conditions,

$$\chi\left(\frac{\pi}{2p}\right) = \begin{Bmatrix} 0 \\ \pi \end{Bmatrix}, \chi\left(\frac{\pi}{2p} + \frac{2\pi}{p}\right) = \begin{Bmatrix} 0 + 2\pi \\ \pi + 2\pi \end{Bmatrix}. \quad (10)$$

We specify the shape of the helical coil's cross section in a plane perpendicular to the reference helical trajectory, introducing normalized orthogonal vectors $(\boldsymbol{t}, \boldsymbol{e}_1, \boldsymbol{e}_2)$, which represent the tangential vector, principal normal, and binormal of the reference helical trajectory $(\boldsymbol{e}_1 = \boldsymbol{t} \times \boldsymbol{e}_2)$. The position of the current filament $\boldsymbol{r}'(\phi, \xi, \eta)$ is given by (see Fig. 5)

$$\boldsymbol{r}'(\phi, \xi, \eta) = \boldsymbol{r}_c(\phi) + \xi \boldsymbol{e}_1(\phi) + \eta \boldsymbol{e}_2(\phi). \quad (11)$$

The direction of the principal normal vector $\boldsymbol{e}_2$ is defined to be outward from the coil center,

$$\boldsymbol{t} = \frac{d\boldsymbol{r}_c}{d\phi} \Big/ \sqrt{\frac{d\boldsymbol{r}_c}{d\phi} \cdot \frac{d\boldsymbol{r}_c}{d\phi}}, \quad (12)$$

$$\boldsymbol{e}_2 = -\frac{\sqrt{A^2\left(\frac{d\chi}{d\phi}\right)^2 + B^2}}{A\left(\frac{d\chi}{d\phi}\right)^2 \epsilon' + B\cos\epsilon} \frac{d\boldsymbol{t}}{d\phi} \quad (13)$$
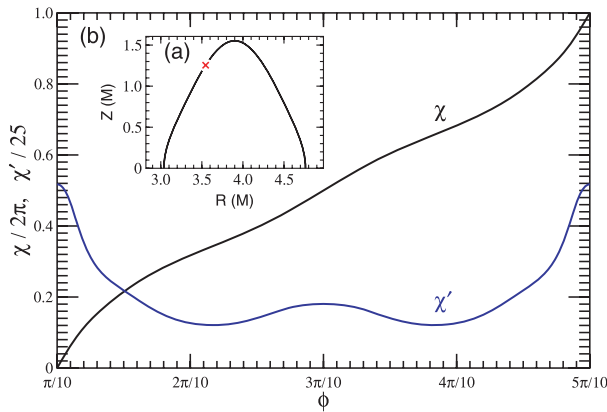
$$(A\cos\epsilon = C', \quad A\sin\epsilon = -B').$$

Fig. 4   (a): Example of a cross section of an elongated ($\kappa = 1.8$) winding frame for helical coils. Position of the reference helical trajectory at $\phi = 0$ is indicated by "×." (b): Variation in poloidal angle χ of geodesic line on the winding frame. One period of the toroidal angle ϕ for the helical coils is $2\pi/5$, because $p = 5$.
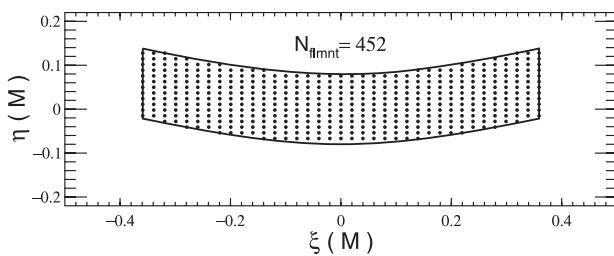

Fig. 5   Example of cross section of helical coils in a plane perpendicular to the reference helical trajectory. Small dots indicate positions of superconducting filaments. Total number of superconducting filament is 452.

In this paper, we use the following model for the minor radius $a(\chi)$,

$$a(\chi) = a_c(1 + a_1\sin^2\chi + a_2\sin^4\chi), \quad (14)$$

and the elongation factor κ of the winding frame of the helical coils is defined as

$$\kappa = 1 + a_1 + a_2. \quad (15)$$

A numerical example for $(a_1, a_2) = (0.3, 0.5)$ is shown in Fig. 4.

A cross section of a helical coil is shown in Fig. 5 for $R_c = 3.9\,\text{m}$, $a_c = 0.865\,\text{m}$, $\kappa = 1.8$, and a coil size of $0.16 \times 0.72\,\text{m}^2$.

3. Characteristics of Magnetic Field Produced by Geodesic Winding Coils

First, we studied the characteristics of the magnetic field produced by the geodesic winding helical coils. When the winding frame is close to circular ($\kappa \simeq 1$), we confirmed the quality of the magnetic surface [D-shaped profile at vertically elongated cross section, $\phi = \pi/10$, large plasma volume, and coexistence of magnetic well (at core plasma region) and high magnetic shear (at peripheral regions)]. However, we found poor performance for a 3.52 MeV alpha particle confinement (see Fig. 3 (b)). Thus, we elongated the winding frame as shown in Fig. 4. The structures of helical coil winding and magnetic surface are shown in Figs. 6 and 7, respectively.

When the elongation factor κ is increased, the magnetic field exhibits a nearly quasi-axi-symmetric configuration rather than helical symmetry (compare Figs. 2 and 7). The 3.52 MeV alpha particle confinement performance is also improved by the elongation of the winding frame (see Fig. 3 (c)). The traces of lost alpha particles on the vacuum vessel are shown in Fig. 8, which shows that their positions are almost the same as the divertor traces of the lines of force.
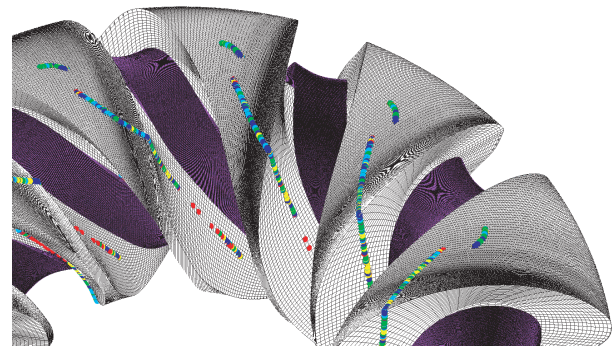

Fig. 6   Vacuum vessel and helical coils of the geodesic winding on an elongated frame ($\kappa = 1.8$). Divertor traces are also shown for the maximum plasma volume. Magnetic surfaces are shown in Fig. 7.

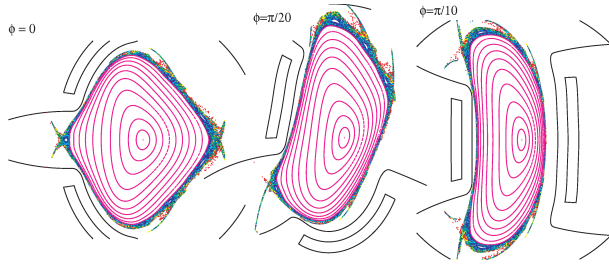Fig. 7 Relationship between magnetic surfaces, vacuum vessel, and helical coils under geodesic winding on a greatly elongated winding frame ($\kappa = 1.8$).
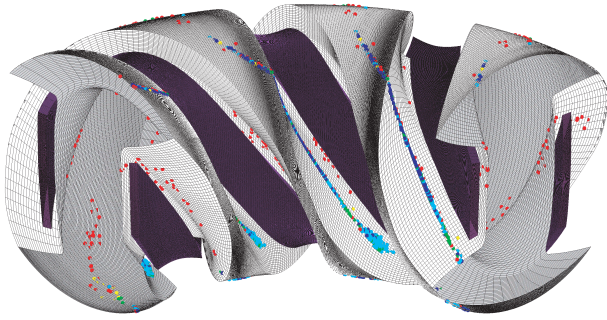

Fig. 8 Traces of 3.52 MeV lost alpha particles on vacuum vessel wall for geodesic winding of helical coils on an elongated winding frame ($\kappa = 1.8$).
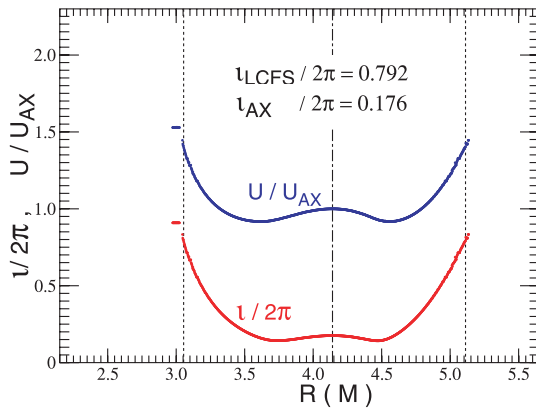

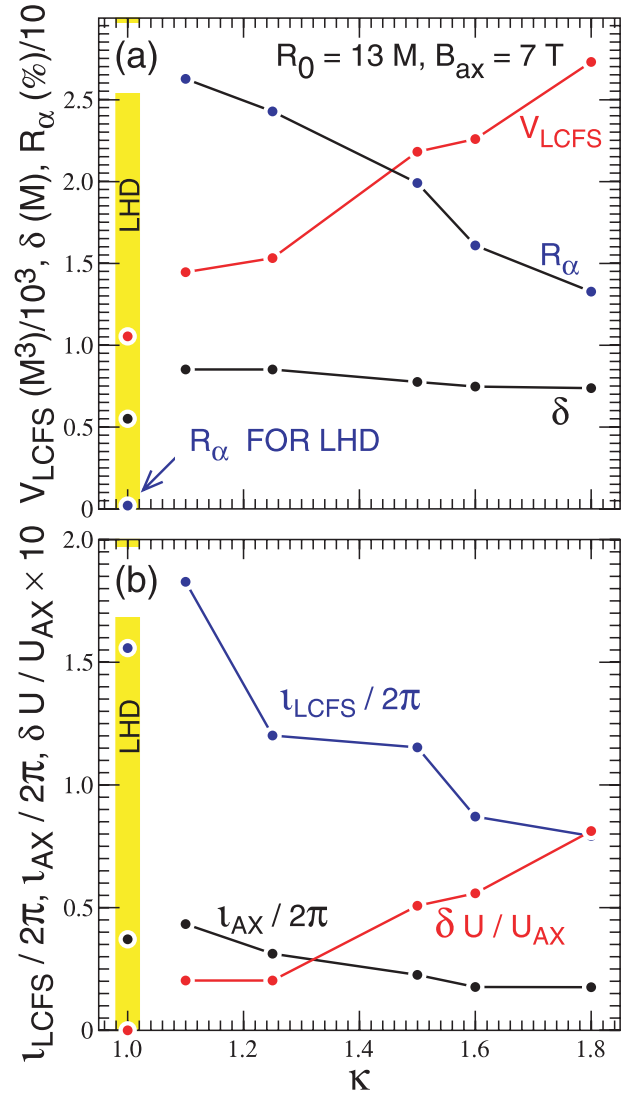Fig. 9 Distribution of rotational transform $\iota/2\pi$ and specific volume U.

Fig. 10 Improvement in characteristics of the magnetic surface with an increasing elongation factor κ of the winding frame for geodesic winding helical coils: (a) magnetic surface volume V_{lcfs}, blanket space δ, and 3.52 MeV alpha particle loss rate R_α, (b) magnetic well depth $\delta U/U_{ax}$, rotational transform $\iota_{lcfs}/2\pi$, and $\iota_{ax}/2\pi$. LHD data are plotted in a yellow hatched region for comparison.

The coexistence of a magnetic well (in the core plasma region) and high magnetic shear (in the peripheral regions) are shown in Fig. 9.

4. Discussion

We proposed a geodesic winding of the helical coils for an LHD-type helical reactor in order to satisfy the requirement for a wide blanket space and large plasma volume in reduced-size helical reactors. Elongation of the cross section of the winding frame of the helical coils improved the confinement of 3.52 MeV DT alpha particles. The improvements in the characteristics of the magnetic surface are summarized in Fig. 10 as a function of the elongation factor κ of the winding frame of the helical coils. The increase in the elongation factor deepens the magnetic well, increases the magnetic surface volume, and decreases the alpha particle loss rate. The geodesic winding of the helical coils with an increased elongation factor κ seems to produce a nearly quasi-axisymmetric magnetic configuration. It is an interesting future subject to examine the limits of the improvement obtained by increasing the elongation factor κ.

For further reduction of the size of a fusion reactor while increasing the blanket space, optimizations of the

functional form $R(\chi)$ and $a(\chi)$ and the helical coil shape (see Fig. 5) are interesting future studies.

DT fusion ignition of a LHD-type helical reactor by Joule heating associated with the magnetic axis position shift have been studied [6]. The D-shaped magnetic surface configuration may be more convenient for current-driven and current-less hybrid operational scenarios in a LHD-type helical reactor owing to the close coupling between the confined plasma and vertical field coil installed inside the helical coils.

In addition, a geodesic winding allows tighter winding of the helical coils. Thus, the helical coil winding is expected to be mechanically stable and easy to manufacture. Furthermore, it has been noted [5] that a geodesic winding is very close to a modulated winding for the force balance coil, which reduced the electromagnetic force on the coils, for a circular winding frame. Reduction of the stress working on the coils mitigates engineering problems in reactor construction. Therefore, the estimation of the electromagnetic force on a geodesic winding of the heli-cal coils on an elongated winding frame is an interesting problem.

[1] N. Ohyabu *et al.*, Nucl. Fusion **34**, 387 (1994).
[2] T. Watanabe *et al.*, Nucl. Fusion **46**, 291 (2006).
[3] T. Mutoh *et al.*, Nucl. Fusion **47**, 1250 (2007).
[4] Y. Kozaki *et al.*, Nucl. Fusion **49**, 115011 (2009).
[5] H. Tsutsui, T. Habuchi, S. Tsuji-Iio and R. Shimada, "Analysis of Stress Distribution in Helical Coils with Geodesic Windings based on Virial Theorem," IEEE Trans. Appl. Supercond. (2011) (in printing).
[6] T. Watanabe, Plasma Fusion Res. **6**, 2405130 (2011).